Preprint 1st June, 2020

Historical large-scale forest dieback and recovery around a copper mine: The case of Ashio Dozan, Japan

Authors

Ruby Mensah and Fumito Koike

Graduate School of Environment and Information Sciences, Yokohama National University, 79-7 Tokiwadai, Hodogaya-ku, Yokohama 240-8501, Japan

Abstract

Acute damage by SO_2 caused large-scale dieback of forest around copper mines before mid-20th century. Although development of technology suppressed SO_2 emission, large-scale degraded lands still remains after half century. We depicted the progress and recovery of dieback since early stage of modern copper mining started at late 19th century in Ashio Dozan based on a historical topographic map and aerial photographs. Degraded lands spread in the early stage of modern mining, and it attained maximum at mid-20th century. Vegetation recovered after that, however 35% of the studied area was still barren land without forest cover. Based on topographic analysis, dieback tend to occurred in valleys and the site with strong solar radiation, probably due to high bulk density of SO_2 gas and its stomatal effect. Recovery occurred sites with large laplacian representing sedimentation with accumulation of soil nutrient and moisture. Further study on wider area covering the whole degraded land, and those based on species composition is necessary because propagule dispersal distance is usually limited and can cause species-poor forest at the center of the large-scale degraded land.

Key words:

Bare land, copper mine, historical ecology, Sulphur dioxide, topographic environment

Introduction

Mining has been regarded as a major catalyst for enhancing development and human welfare both in developed and developing nations (UNDP, 2016). Despite the contribution of mining to socio-economic development, its effect to the natural environment cannot be over looked (Mudd et al, 2013).

Mining causes three types of large-scale environmental damages. One is surface mining developed recently as a cost efficient technique for low quality ores. Surface mining poses threat to terrestrial ecosystems by removing entire ecosystem and topography at the mining sites completely, and caused irreversible changes on ecological landscapes (Tischew et al 2014; Slonecker & Benger 2001; Hendrichová & Kabrna 2016). However, these effects are mostly limited to inside the mining site. Another effect is by water pollution. Metals, some toxic elements and acids dispersed by water and cause large-scale damages on ecosystems including agricultural pollution in downstream of river (Hu et al 2016). The last one is by air pollution. Some metal ores as copper pyrite contain sulfide. Smelting and refining process produces SO_2 gas. The gas was diffused by air and damaged forests surrounding large areas around the mine (Anna et al. 2011). It damaged all plants from trees to mosses in wide region, and as consequence it leaded severe soil erosion. Although emission of SO_2 has been eliminated due to development of smelting and refinery technology in mid-20th century, large scale barren land still exist.

Scientific studies on the recovery of these large-scale damaged land is limited (Holl 2002), and those on historical dieback by copper mining is quite rare. In this paper, we depicted the progress in forest dieback in the development of copper mining in early 20th century, and following forest recovery using a historical map and aerial photographs around the center of Asio Dozan copper mine located in temperate Japan.

Materials and Methods

History of mine and SO_2 emission

The studied copper mine, Ashio Dozan mine (latitude 139.437ºE and longitude 36.633ºN), located in a valley (700 m in altitude) in Ashio Mountains. It is in the upper reaches of the Watarase River in western Tochigi prefecture, 120 km Northwest of Tokyo. Underground mining in Bizentate Mountain (1272 m in altitude) was major ways to obtain ores as chalcopyrite ($CuFeS_2$), although several ancient open pit remains were found (Fig. 1).

Ashio Dozan copper mine has long history since 17th century (Murakami 2006) (Fig. 2). In the industrial revolution of Japan, copper mining was the backbone of the Japanese economy as it played a major role in Japans capitalism (about 10% to GDP as of 1890) with the main domestic producer being the Ashio Dozan mine (Shoji and Sugai, 1992). Copper production increased since 1880s and attained the maximum in 1917. It decreased by the World War II, and recovered 1960s. The mine was closed in 1973 due to exhaustion of ores. Copper production using imported ores by smelting and refining facilities in Ashio Dozan became large amount in 1960s. All smelter and refinery were stopped in 1989 (Murakami 2006).

The emission of SO_2 gas can roughly assumed as parallel to copper production before flash smelting was introduced in 1956 (Fig. 1). Air pollution became significant social issue in 1897, although key technology to suppress SO_2 emission was lacking. The possible measure was to discharge SO_2 when wind did not bound for the major cities, Tsudo (Fig. 1) and Nikko (east of the area), based on weather observations (Murakami 2006). SO_2 gas emission decreased after 1956 by applying flash smelting, and the new environmental standard was satisfied in 1975 (Fujii et al 1981). Major smelter and refinery located in Honzan and Kotaki areas in the early period of modern mining (Fig. 1). After the smelter and refinery in Kotaki was closed in 1897, those in Honzan became the major source of SO_2 emission (Murakami 2006).

History of forest

All research areas belong to cool-temperate deciduous broadleaf forest biome (Environment Agency http://gis.biodic.go.jp/webgis/sc-009.html) with mean annual temperature 6.9 °C and annual precipitation 2176 mm/year at the closest metrological station Oku-Nikko at altitude 1292 m (https://www.data.jma.go.jp 2019/11/25). The mine area was covered by forests at the beginning of modern mining, and forest damages by early-modern mining might be recovered at that time (Murakami 2006).

By mining activities, forests were harvested for woods supporting mine tunnel, and fuels for smelting and refining in the early period of modern mining (Fig. 2). SO_2 emission also damaged forests, and large forest fire was also recorded in this period. Forest reduction caused floods in downstream, and forest conservation became significant social issue in addition to air pollution. Forest harvest was prohibited in this region since 1897 (Murakami 2006). The next forest harvest was around the World War II due to deficit for home livelihoods. The forest recovery activities continued since 1897 and it is still on going in 2010s (Nakamura and Shimomura 2009; Aoki and Nagai 2010).

Land cover data

We set 5.4 km (west-east) × 6.6 km (south-north) study area to analyze land cover around Bizentate Mountain locating at the center of the mine (Fig. 1). The studied area was mountainous, the altitude is 885 ±152 m (average ± SD) and slope is 37.0 ±11.6 degree (Fig. 3).

We examined land cover in the early stage of modern mining (period I in Fig. 2) and the last stage of modern mining before satisfying current environmental standard (period II in Fig. 2) to evaluate the progress of forest dieback due to air pollution. We compared period II to the stage after current environmental standard was satisfied (period III in Fig. 2) to evaluate forest recovery.

Forest harvests cause deforestation, in addition to the dieback by air pollution. Usually young forest recovers within 20 years from the harvest (Fukamach and Nakashizuka 2001), if continuous suppressor, as air pollution, is lacking (Fig. 5). In order to distinguish the effect by air pollution from forest harvesting and temporal bare-land by forest fire, we examined land cover data at two points of time departed at least 20 years, and the maximum thickness of vegetation (0: bare-land, 1: grassland and scrubland, 2: sparse forest, and 3: dense forest) was considered as the land cover of the period.

The first data on the land cover of this region is 1:50000 topographic map with information on vegetation. The study area is covered by two maps Ashio surveyed in 1907 and Nantaisan in 1912 (Geographic survey institute 1912, 1915). Two maps were connected into one land cover data in 1907-1912. Since older map does not exist, period I has only one data (Fig. 2). We examined two aerial photographs taken in 1948 and 1969 for period II, and 1985 and 2014 for period III (Geographical Survey Institute http://mapps.gsi.go.jp/ maplibSearch.do#1 2019/4/8).

In order to examine transition of land cover, 396 study points (300 m intervals, 18 in west-east × 22 in south-north) were set covering the study area (Fig. 1). These points were overlaid on the georeferenced historical map and aerial photographs by a GIS software (Koike 2019). Vegetation thickness was examined by eyes at each point on map and photographs and entered to the GIS file using data input function of the software (Table 1).

The barren land on the topographic map include bare-land, grassland and scrubland, so we combined these land covers in the analysis of dieback from period I to II, and assign vegetation thinness index of barren land to be 0.5. The topographic map also did not distinguish sparse forest from dense forest, so we combined these land covers in the analysis of dieback process, and assigned the value 3 for the forests on the topographic map. Rivers, roads, villages, cultivated lands, and obscured points by clouds were excluded from analysis.

Data analysis

In order to analyze forest dieback, we divided three grades of damage. When the land was barren throughout periods I to II, the damage grade 2 was assigned to the study point. When damage progressed (forest in period I and barren land in period II), the damage grade to be 1, and the damage grade 0 if land was forest throughout periods I to II. Generalized linear model (R version 3.5.1) was applied assuming the damage grade to be objective variable, and explanatory variables as slope inclination, slope laplacian, horizontal open angle, solar radiation, logarithm transformed specific catchment area, and geographical coordinate as x (west to east), x^2, y (south to north), and y^2.

Laplacian represents concavity of terrain. Positive values mean soil sedimentation, and negatives mean erosion. Horizontal open angle is the percentage in horizontal angle without higher altitudinal terrain surrounding the focal study point. The value is zero in a valley bottom surrounded by ridges, and 100% at the top of highest summit with good ventilation. Solar radiation and specific catchment area represents xeric and mesic environments for plants. The geographical coordinate x and y were entered to consider the position of SO_2 source as the smelter and refinery. Topographical variables as slope inclination, laplacian, horizontal open angle, solar radiation, and specific catchment area were obtained from 50 m mesh digital elevation model by Geographical survey institute (2001) using the GIS software (Koike 2019) (Fig. 3).

In order to analyze recovery from forest dieback, we considered 145 study points where barren land continued throughout the period I and II (Fig. 2). For these study points, degree of recovery was assigned as zero if the study point was barren land at period III. It was 1 if forest was recovered to forest in the period III. Generalized linear model (R 3.5.1) was applied assuming the recovery grade to be binary objective variable, and explanatory variables as slope inclination, slope laplacian, horizontal open angle, solar radiation, logarithm transformed specific catchment area.

Results

Land cover at each point of time

Barren land covered 48% of examined points at the time of 1907-1912 map (Fig. 6), and it peaked at 60% in 1948. After that it decreased gradually to 1969, and rapidly after 1970s coincide with increase in forest cover. It covered 35% of the tested points, and 65% was covered by forest as of 2014.

At the period I in early stage of modern mining (Fig. 2), large barren land was found along Matsugi River locating Honzan smelter and refinery on the 1907-1912 map (A in Fig. 7). Another large barren land existed along Koushin River locating Kotaki smelter and refinery (B). Other barren land patches were found on the hill in south-eastern side of Watarase River distant from smelter and refinery (C).

At the period II as the last stage of modern mining, the barren land B along Koushin River and C disappeared in 1948, whereas new barren land D was found in upstream of Nitamoto River and E in the north-west side of Tsudo. This pattern was basically similar in 1961.

At the period III after the current air pollution standard was satisfied, gradual recovery was found in the degraded area. Small scale degradations scattered in the southern part of study area (F and G in Fig. 7)

Progress of dieback and recovery

Large barren land continued from the beginning (period I) to the end (period II) of modern copper mining locating around Matsugi River, and smelter and refinery at Honzan was in this area (Fig. 8). New barren land was formed after period I at west-side of this large barren land. The summit and western slope of Bizentate Mountain was covered by forest throughout modern mining, although it located at the center of Ashio Dozan mine. Geographical coordinates were significant, and location was an important factor in the process of dieback (Table 2). Horizontal open angle contributed negatively, and dieback occurred in valley. Solar radiation promoted dieback.

Forest recovery after period II (Fig. 2) was detected in the marginal area of large barren-land observed in period II (Fig. 9). Topographical laplacian was positive factor for recovery (Table 3).

Discussion

Forest dieback and its recovery history was depicted quantitatively around the center of Ashio Dozan copper mine (Fig. 6). Large barren-land was formed at the beginning of modern mining (period I). It enlarged even after the early environmental protection measures had been taken in

1897 (Fig. 8), and enlarged until the last stage of modern mining (period III). The peak of damaged was in mid-20th century.

The damaged area responded to the shift of mine facilities. The barren land along Koushin River in the period I may be due to the pollution by Kotaki smelter and refinery, although forest recovered after the smelter was closed and integrated to Honzan (B in Fig. 7). The remaining record of forest damage (Matsuura and Ishii 2010) confirms the history of this dieback area.

On the other hand deforestation and recovery occurred in small spatial and temporal scales on the south-eastern side of Watarase River. Barren lands might not always corresponded to the air pollution (C, G and F in Fig. 7), though these areas were also reported as slightly damaged by air pollution (Ichikawa 1956). Historical information suggests that woods in national forest around the site C were harvested and sold to the mine (Matsuura and Ishii 2010; Aoki and Nagai 2010), and such harvest might affect deforestation.

Topography affected forest dieback and recovery. Dieback was severe in the valley with low value in horizontal open angle (Table 2), and the summit had limited damage probably due to better ventilation. Heavy bulk density of SO_2 (2.63 kg/m^3 against 1.293kg/m^3 of air) might flow along valleys and caused severe damage in those sites. Strong solar radiation might cause heat and water stresses for plants with difficulty in opening and closing of stomata by SO_2 (Black and Unswrth 1980).

Forest dieback distributed to northern area from the center of emission at Honzan (Fig. 8). The mine controlled the discharge of SO_2 depending on wind direction to avoid effect on Tsudo area with much human population. This caused pollution in northern upstream of Matsugi River. The mine also avoided to effect Nikko area locating east after 1897 (Murakami 2006), and such control might cause new damages in western side of the old damaged area in the period between I and II (Fig. 8).

Significant forest recovery occurred after the end of emission, although large barren lands remains still in 2014 (Fig. 9). Forest recovered at the site with high laplacian, suggesting concaved topography with soil sedimentation (Table 3). Such sites can be rich in soil moisture and nutrients eroded from convex topography (Zhuab et al 2015).

Because we aimed to analyze core area of Ashio Dozan mine, we did not studied barren land in northern area distant from the center of the mine. Studies covering the whole damaged area is needed in future to depict the whole history of dieback and recovery. Sensitivity to SO_2 gas differs by species (Steubing and Fangmeier 1987). Seed dispersal distance by bird is usually less than 500 m (Komuro and Koike 2005), and propagule limitation will cause delay in recovery at the center of large-scale barren land (Ohtani and Koike 2002). Species-explicit community level study is needed for recovery of large scale barren land and physiognomically recovered forests.

Acknowledgements

The authors thank staffs of Ashio Branch, Nikko Municipal Office for their all kinds of supports, Donryuji temple for providing accommodation and kind supports in staying Ashio Town.

Reference

Aoki T, Nagai M 2010. The historical transition of rehabilitation and reforestation in degraded lands in Ashio copper mine: A consideration about the relationship among conservation, restoration and utilization of Matsugi District. Proceedings of JSCE series D 66: 197-216

Black VJ, Unswrth MH 1980. Stomatal responses to sulphur dioxide and vapour pressure deficit. Journal of Experimental Botany 31: 667–677.

Fujii O, Shima M, Nakao S 1981. Copper smelting and the by-product plants in Ashio Smelter. Nihon Kogyokai-si 97: 627-632

Fukamachi, K., Oku, H. & Nakashizuka, T. 2001. The change of a satoyama landscape and its causality in Kamiseya, Kyoto Prefecture, Japan between 1970 and 1995. Landscape Ecology 16: 703-717.

Geographic survey institute 1912. 1:50000 map Ashio. Geographic survey institute, Tsukuba.

Geographic survey institute 1915. 1:50000 map Nantaisan. Geographic survey institute, Tsukuba.

Geographical survey institute 2001. Digital map 50 m grid (elevation) II. Geographical survey institute, Tsukuba.

Hendrychová M, Kabrna M 2016. An analysis of 200-year-long changes in a landscape affected by large-scale surface coal mining: History, present and future. Applied Geography 74: 151-159.

Holl KD 2002 Long-term vegetation recovery on reclaimed coal surface mines in the eastern USA. Journal of Applied Ecology 39: 960-970

Hu YN, Cheng HF, Tao S 2016 The challenges and solutions for cadmium-contaminated rice in China: A critical review. Environmental International 92-93: 515-532

Ichikawa M 1956 A study on the wasted land and the debris supply from the bare land slopes in the upper drainage area of the Watarase. Geographical review of Japan 29: 38-52.

Koike F 2019 Minna de GIS. http://www.minnagis.com

Komuro, T. and Koike, F. 2005. Colonization by woody plants in fragmented habitats of a suburban landscape. Ecological Applications 15: 662-673.

Matsuura S, Ishii S. 2010. Ashio sanchi niokeru kodoku mondai. Water science 54: 58-78. https://doi.org/10.20820/suirikagaku.54.4_58 (Pollution issue in Ashio Mountains)

Mudd GM, Weng Z, Jowitt SM 2013 A detailed assessment of global Cu resource trends and endowments. Economic Geology : 1163-1183.

Murakami Y 2006 Ashio Dozan-si. Zuisousha, Utunomiya. (History of Ashio Dozan mine)

Ohtani, S. and Koike, F. 2005. Implications of 19th-century landscape patterns for the recovery of Fagus crenata forests. Applied Vegetation Science 8: 125-132. DOI: 10.1111/j.1654-109X.2005.tb00637.x

The R Foundation for Statistical Computing 2018 R version 3.5.1.

Shoji and Sugai, 1992. Tsushi Asio kodoku jiken 1877-1984. Seorishobo, Yokohama. (History of pollution issue in Ashio 1877-1984)

Steubing L and Fangmeier A 1987 SO_2-sensitivity of plant communities in a beech forest. Environmental Pollution 44: 297-306

Slonecker ET & Benger ML 2001. Remote sensing and mountaintop mining. Remote Sensing Reviews 20: 293-322

Tischew S, Baasch A, Grunert H, Kirmer A 2014. How to develop native plant communities in heavily altered ecosystems: examples from large-scale surface mining in Germany. Applied Vegetation Science 17: 288-301

UNDP, 2016

Zhuab Q, John P.Schmidtc JP, Bryantb RB 2015 Maize (Zea mays L.) yield response to nitrogen as influenced by spatio-temporal variations of soil–water-topography dynamics. Soil and Tillage Research 146: 174-183

Table 1. Land cover expression based on historical topographic map and aerial photograph. Vegetation thickness index are in parentheses.

Vegetation category	Historical topographic map	Aerial photograph
Barren land	Barren land (0.5)	Bare land (0)
		Grassland and scrubland (1)
Forest	Broad leaf forest, coniferous forest (3)	Sparse forest (2)
		Dense forest (3)
Not analyzed	River, road, village, cultivated lands	River, road, village, cultivated lands

Table 2. Factors determining forest dieback in modern mining. Dieback from period I to II was analyzed (Fig. 2). Variables were selected based on AIC.

Variable	Estimate	SD	t-value	P	
Intercept	21.3	58.6	0.363	0.717	
Horizontal open angle	-2.09	0.59	-3.544	0.000453	***
Solar radiation	1.42×10^{-04}	4.27×10^{-05}	3.315	0.00102	**
Geographical position					
x	-11.4	1.11	-10.255	$<2.0 \times 10^{-16}$	***
x^2	-0.162	0.0158	-10.252	$<2.0 \times 10^{-16}$	***
y	-6.39	1.51	-4.233	3.03×10^{-5}	***
y^2	0.0459	0.0105	4.391	1.54×10^{-5}	***

Table 3. Factors determining recovery of forest from the barren lands after the last period of modern mining. Recovery from period II to III was analyzed (Fig. 2). Variables were selected based on AIC.

Variable	Estimate	SD	z value	P	
Intercept	1.34	1.15	1.17	0.242	
Laplacian	1.68	0.568	2.95	0.00317	**
Horizontal open angle	5.59	3.10	1.80	0.0714	.
log Specific catchment area	-0.293	0.209	-1.40	0.160	

Figure legends

Fig. 1 Map of studied area. Dots represent the position where transition of land cover is examined. Background map is current 1:25000 topographic map (Geographical Survey Institute, https://maps.gsi.go.jp/).

Fig. 2 History of copper production in Ashio Dozan mine (Murakami 2006). Arrows represent the point of time at land cover was examined by a topographic map and photographs.

Fig. 3 Topographic variables used in analysis. Rectangular represents studied area. Brightness represent larger value in each variable, excluding legalism of catchment area showing inverse in brightness.

Fig. 4 Maps and aerial photographs analyzed.

Fig. 5 Hypothetical diagram showing the method to distinguish pollution effects from ordinal forest harvesting.

Fig. 6 Changes in percentage land cover of forest (dense and sparse forest) and barren land (bare land, grassland and scrub land) in examined points.

Fig. 7 Map of examined points and distribution of forest and barren land. Background map is current 1:25000 topographic map (Geographical Survey Institute, https://maps.gsi.go.jp/).

Fig. 8 Progress of dieback from early stage (period I in Fig. 2) to the end of modern mining (period II). Background map is historical 1: 50000 topographic map by Geographical Survey Institute (1912, 1915).

Fig. 9 Forest recovery from the end of modern mining (period II in Fig. 2) to after the new environmental standard was attained (period III). Background map is historical 1: 50000 topographic map by Geographical Survey Institute (1912, 1915).

Fig. 1

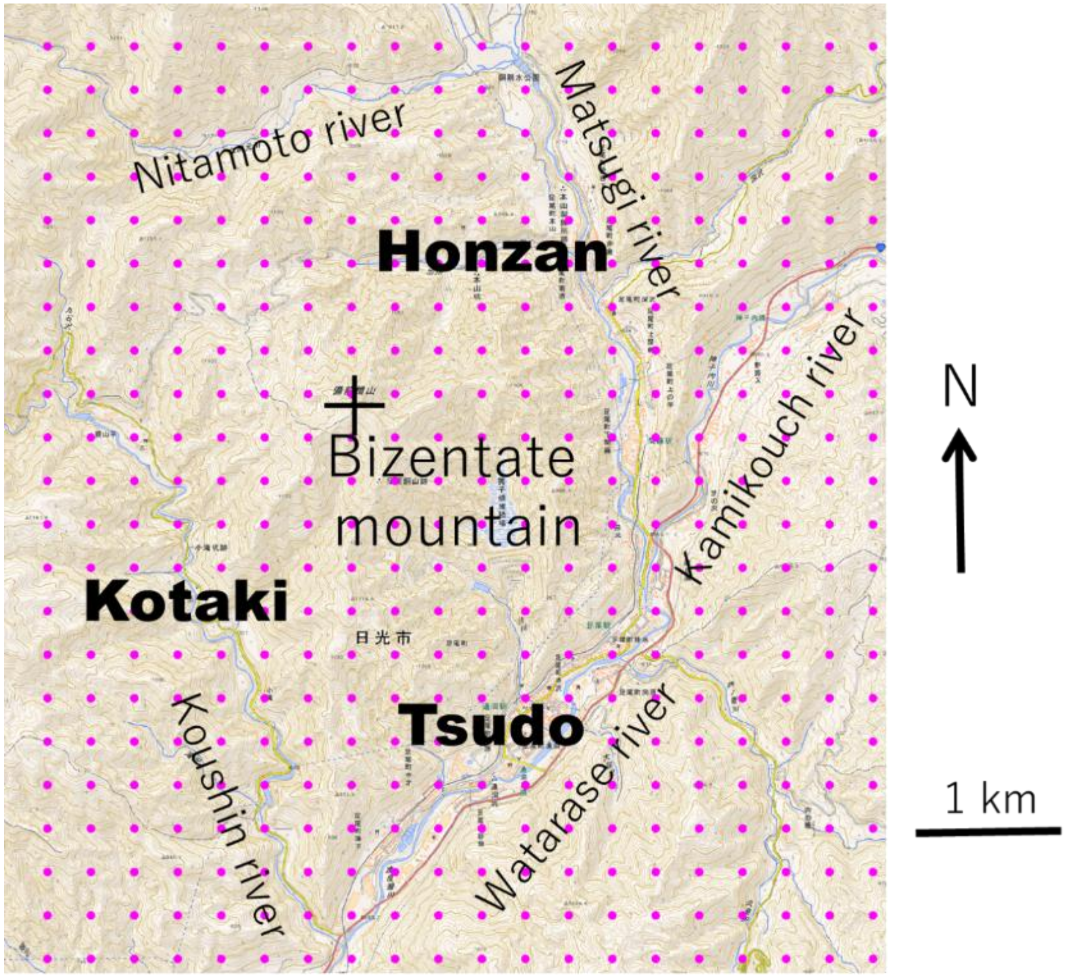
Nitamoto river
Matsugi river
Honzan
Kamikouch river
Bizentate
mountain
Kotaki
日光市
Tsudo
Koushin river
Watarase river
N
1 km

Fig. 2

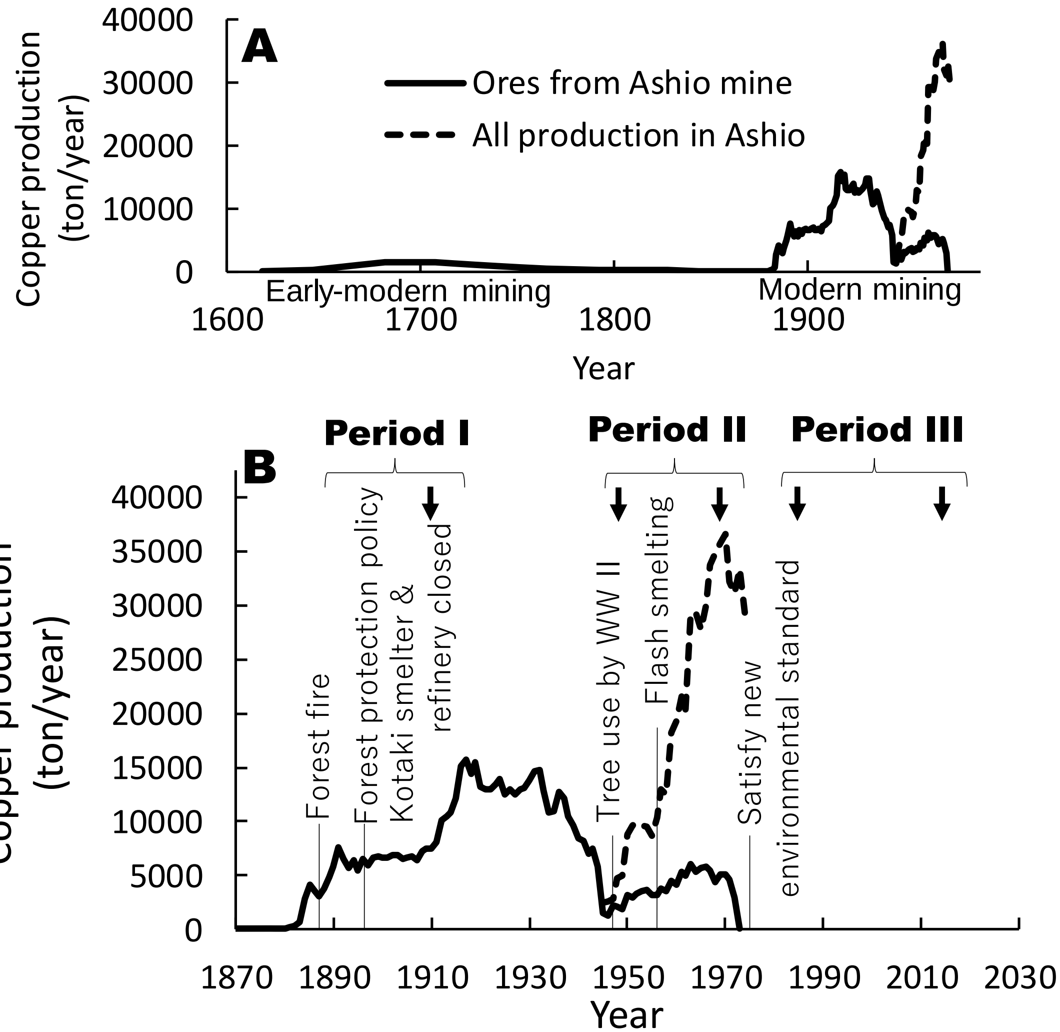
A
Ores from Ashio mine
All production in Ashio
Copper production (ton/year)
40000
30000
20000
10000
0
Early-modern mining
Modern mining
1600
1700
1800
1900
Year
Period I
Period II
Period III
B
Forest fire
Forest protection policy
Kotaki smelter & refinery closed
Tree use by WW II
Flash smelting
Satisfy new environmental standard
Copper production (ton/year)
40000
35000
30000
25000
20000
15000
10000
5000
0
1870
1890
1910
1930
1950
1970
1990
2010
2030
Year

Fig. 3

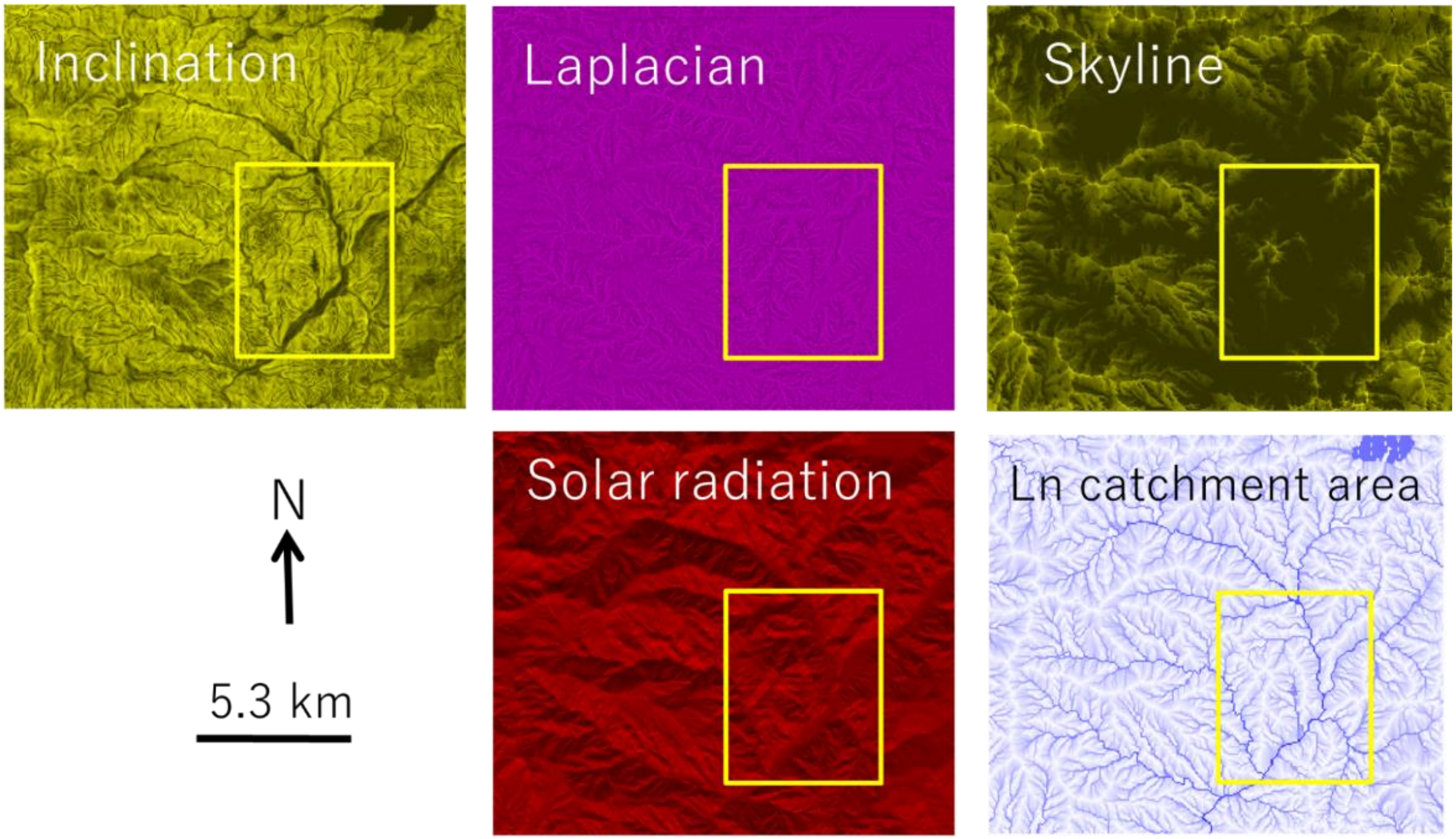

Inclination
Laplacian
Skyline
N
5.3 km
Solar radiation
Ln catchment area

Fig. 4

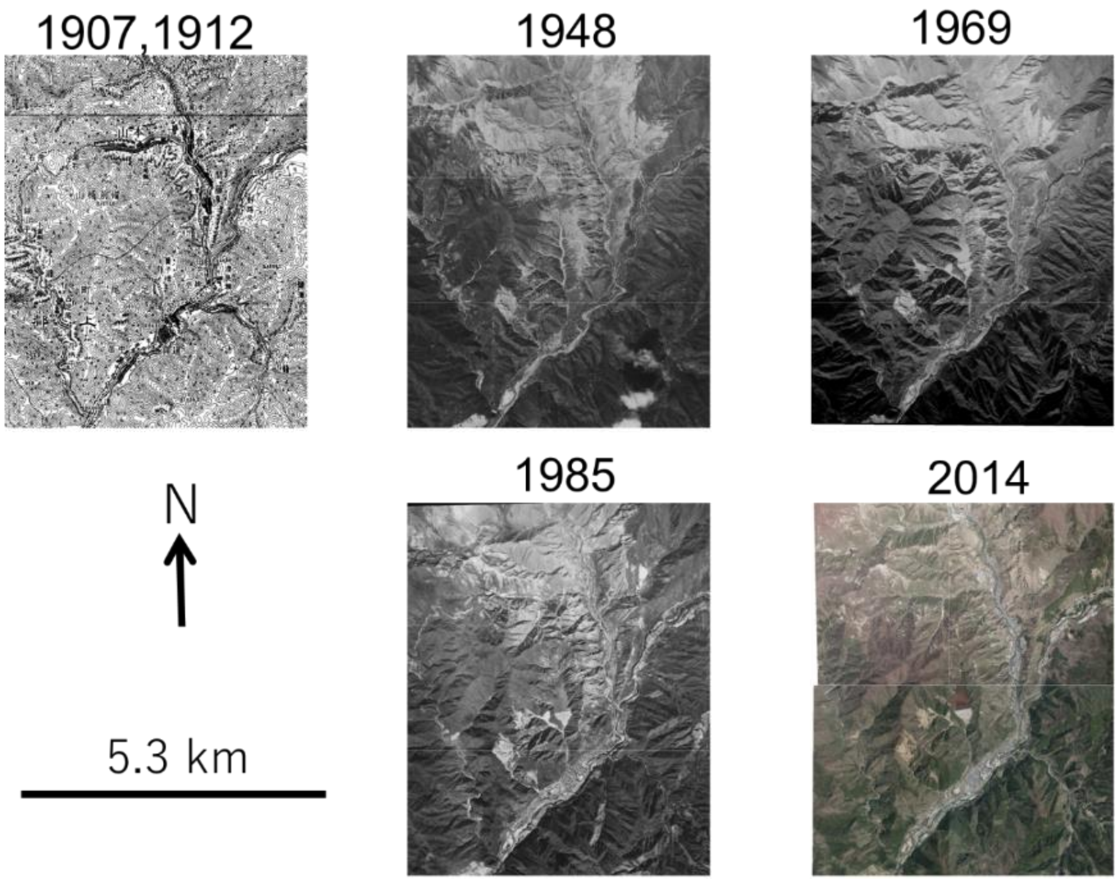

Fig. 5

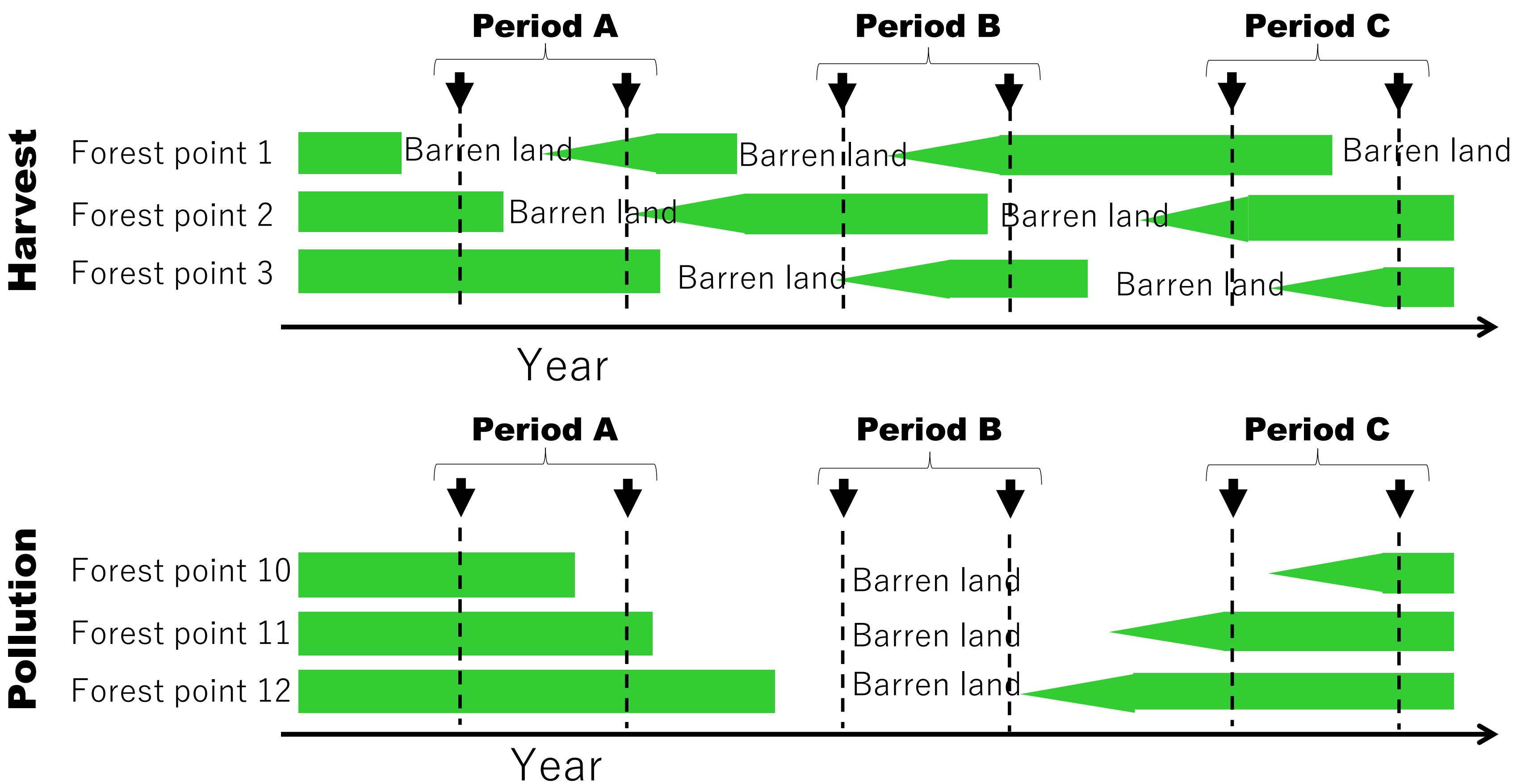

Period A
Period B
Period C
Harvest
Forest point 1
Forest point 2
Forest point 3
Barren land
Barren land
Barren land
Barren land
Barren land
Barren land
Barren land
Year
Period A
Period B
Period C
Pollution
Forest point 10
Forest point 11
Forest point 12
Barren land
Barren land
Barren land
Year

Fig. 6

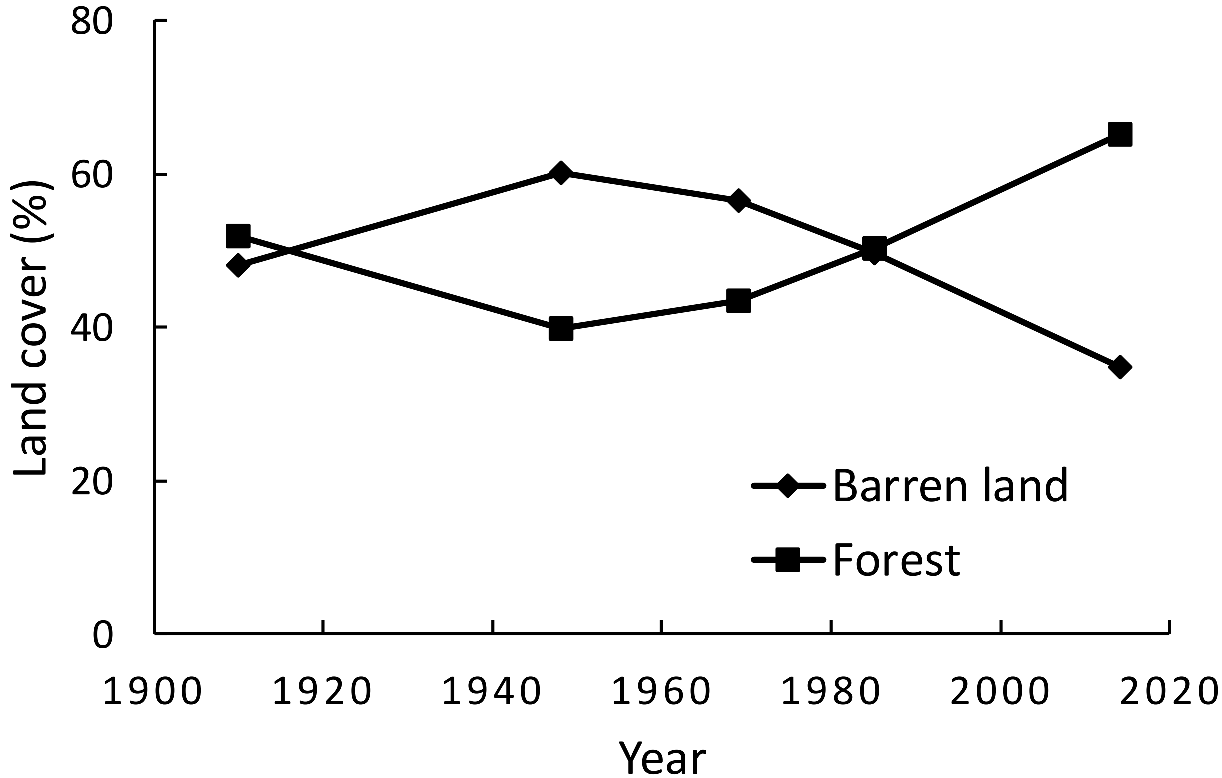

80
60
40
20
0
Land cover (%)
1900
1920
1940
1960
1980
2000
2020
Year
Barren land
Forest

Fig. 7

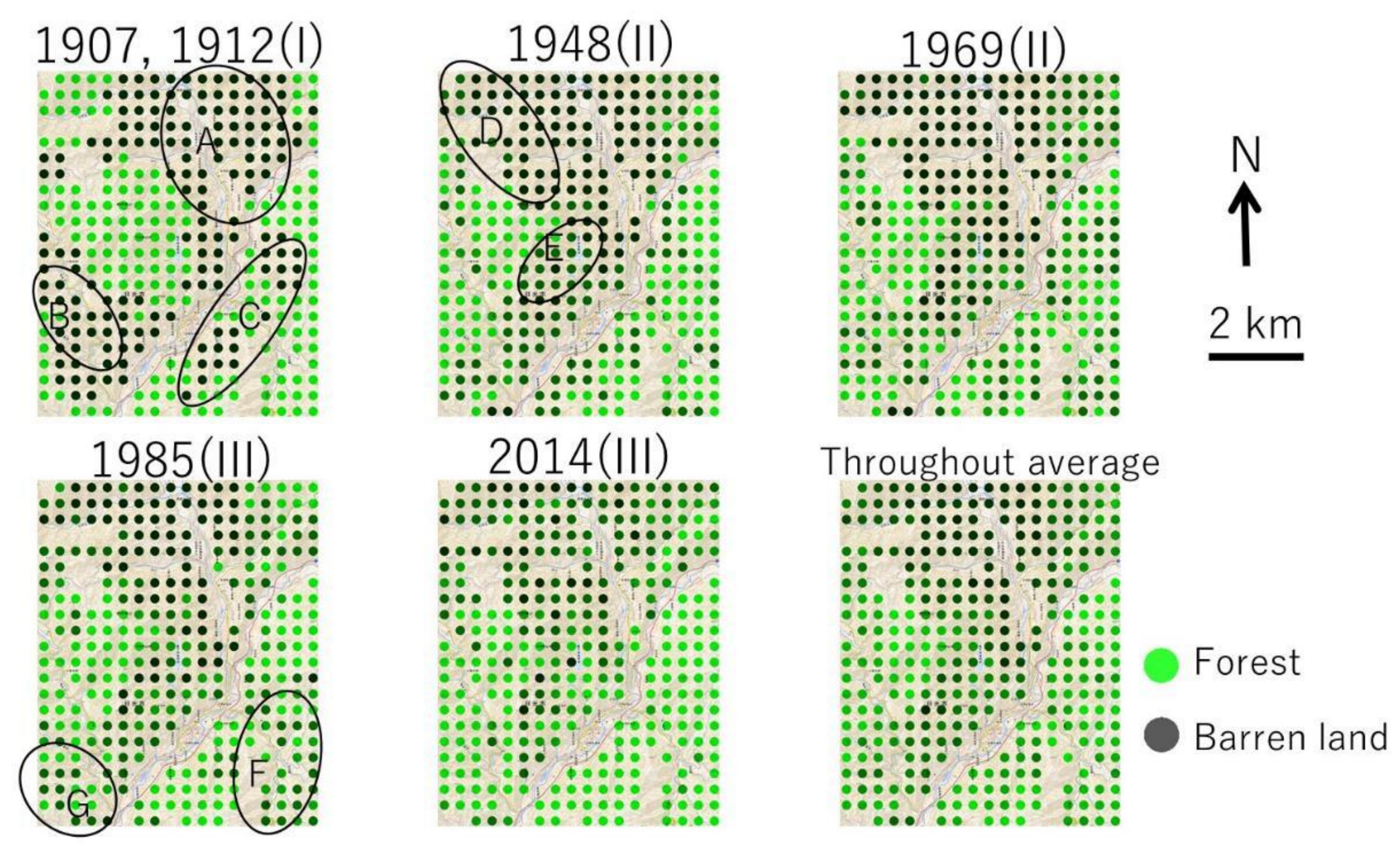
1907, 1912(I)
1948(II)
1969(II)
1985(III)
2014(III)
Throughout average
A
B
C
D
E
F
G
N
2 km
Forest
Barren land

Fig. 8

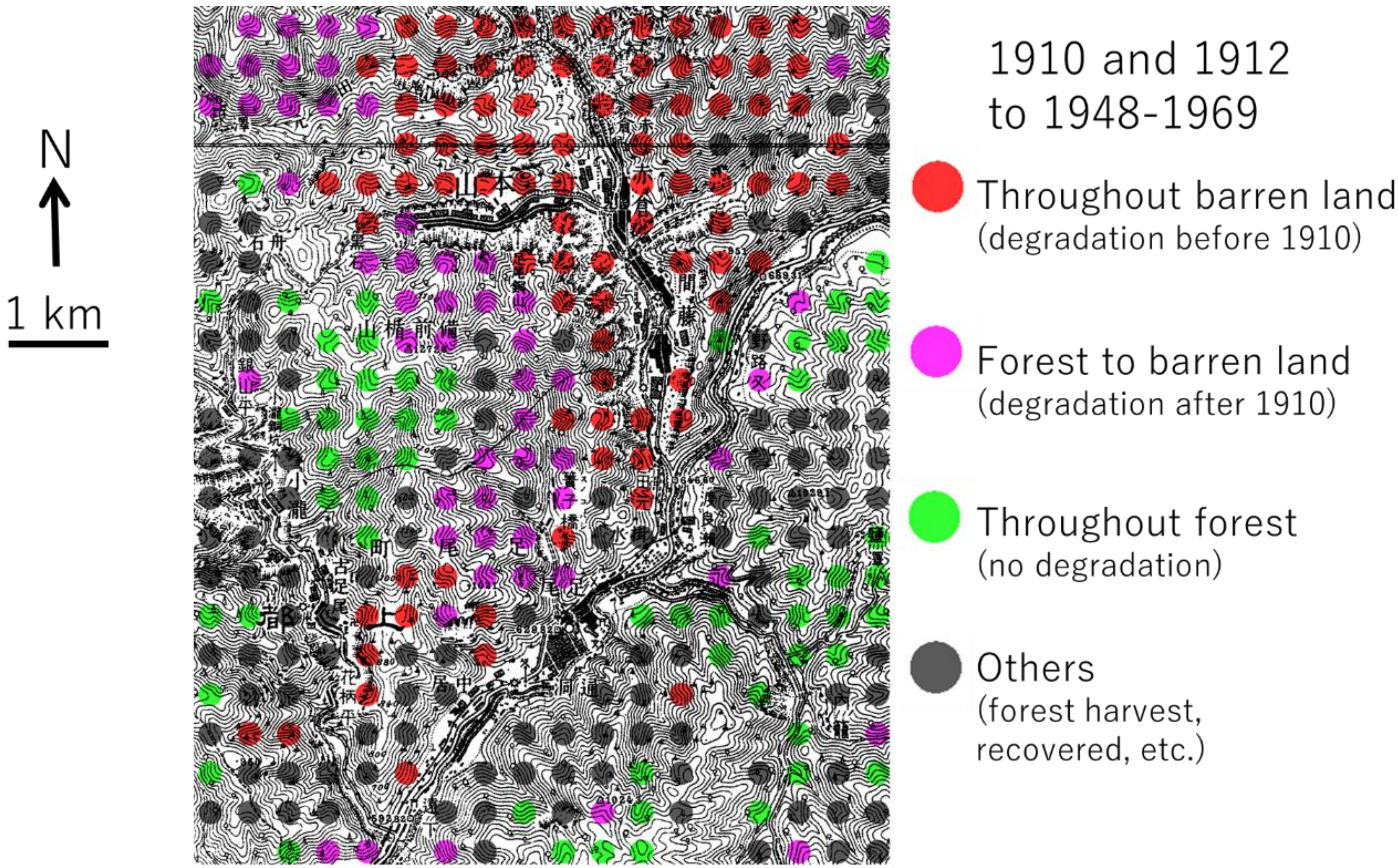
N
1 km
1910 and 1912
to 1948-1969
Throughout barren land
(degradation before 1910)
Forest to barren land
(degradation after 1910)
Throughout forest
(no degradation)
Others
(forest harvest,
recovered, etc.)

Fig. 9

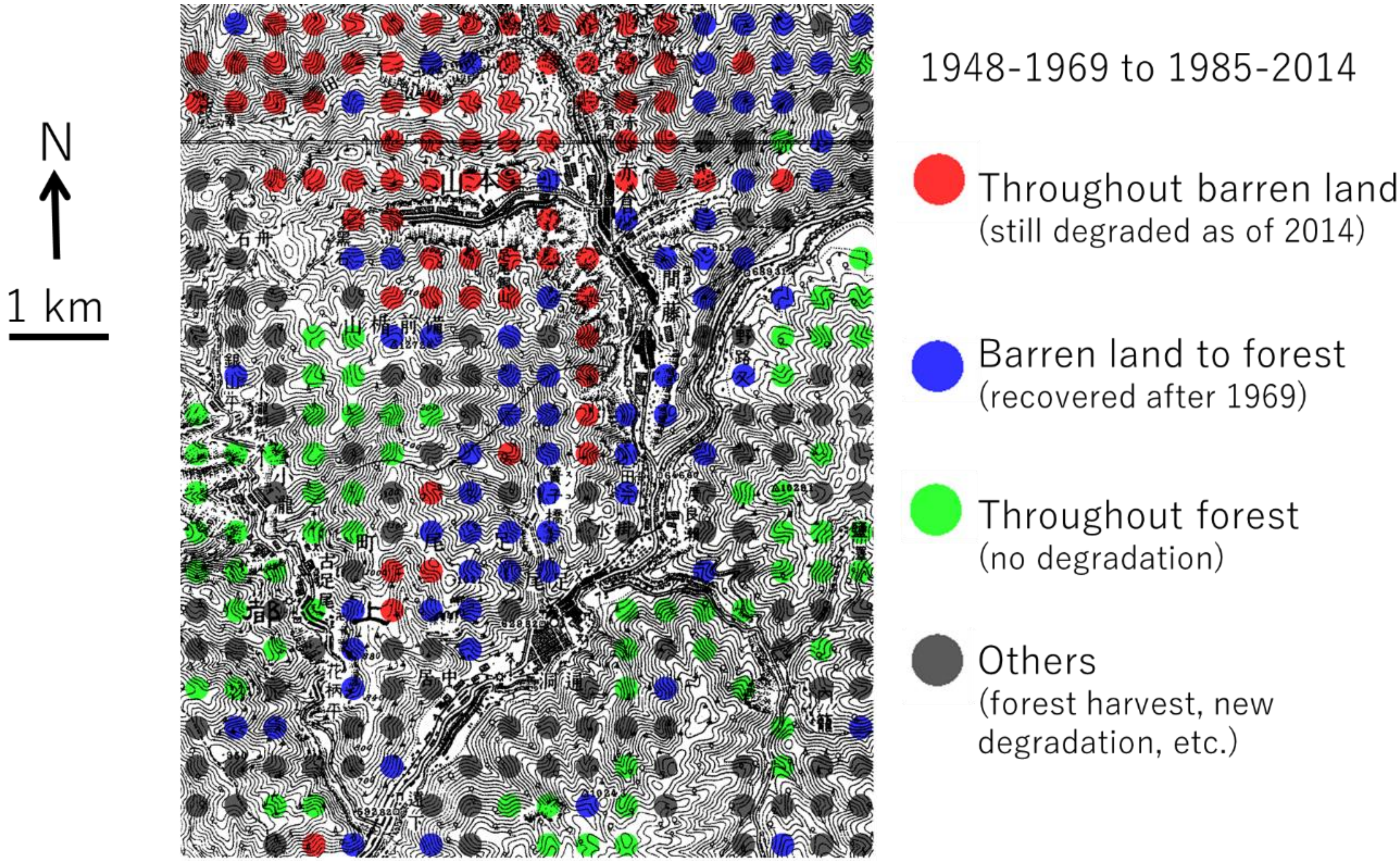
N
1 km
1948-1969 to 1985-2014
Throughout barren land
(still degraded as of 2014)
Barren land to forest
(recovered after 1969)
Throughout forest
(no degradation)
Others
(forest harvest, new degradation, etc.)